

# Investigation of the spin state of Co in LaCoO<sub>3</sub> at room temperature

S.K. Pandey,<sup>1,4</sup> Ashwani Kumar,<sup>2</sup> S. Patil,<sup>1</sup> V.R.R. Medicherla,<sup>1</sup> R.S. Singh,<sup>1</sup> K. Maiti,<sup>1</sup> D. Prabhakaran,<sup>3</sup> A.T. Boothroyd,<sup>3</sup> and A.V. Pimpale<sup>4</sup>

<sup>1</sup>*Department of Condensed Matter Physics and Materials Science,*

*Tata Institute of Fundamental Research, Homi Bhabha Road, Colaba, Mumbai - 400 005, INDIA.*

<sup>2</sup>*Department of Physics, Institute of Science and Laboratory Education, IPS Academy, Indore 452 012, India.*

<sup>3</sup>*Clarendon Laboratory, Department of Physics, University of Oxford, Parks Road, Oxford OX1 3PU, UK.*

<sup>4</sup>*UGC-DAE Consortium for Scientific Research, University Campus, Khandwa Road, Indore 452 017, India.*

(Dated: October 27, 2018)

We investigate the spin state of LaCoO<sub>3</sub> using state-of-the-art photoemission spectroscopy and *ab initio* band structure calculations. The GGA+*U* calculations provide a good description of the ground state for the experimentally estimated value of electron correlation strength, *U*. In addition to the correlation effect, spin-orbit interaction is observed to play a significant role in the case of intermediate spin and high spin configurations. The comparison of the calculated Co 3*d* and O 2*p* partial density of states with the experimental valence band spectra indicates that at room temperature, Co has dominant intermediate spin state configuration and that the high spin configuration may not be significant at this temperature. The lineshape of the La 5*p* and O 2*s* core level spectra could be reproduced well within these *ab initio* calculations.

PACS numbers: 71.20.-b, 75.20.Hr, 71.27.+a, 79.60.Bm

## I. INTRODUCTION

The evolution of the spin state of Co in LaCoO<sub>3</sub> with temperature has drawn a great deal of attention during last 50 years.<sup>1,2,3,4,5,6,7,8,9,10</sup> The ground state of this compound is believed to be nonmagnetic (spin  $S = 0$ ) insulator. It shows two magnetic transitions at about 100 K (a sharp transition) and at around 500 K (broad).<sup>11</sup> The second transition is also accompanied by an insulator to metal transition. All these magnetic transitions have been attributed to the temperature induced spin state transition of Co<sup>3+</sup> ions. Initially it was believed that the transition at 100 K occurs due to the change in the spin state of Co<sup>3+</sup> ion from low spin (LS) state ( $t_{2g}^6 e_g^0 \Rightarrow S = 0$ ) to a mixed LS and high spin (HS) states ( $t_{2g}^4 e_g^2 \Rightarrow S = 2$ ).<sup>1,3</sup> In order to achieve a microscopic understanding of these transitions, photoemission spectroscopy (PES) and *x*-ray absorption spectroscopy (XAS) have been employed extensively, since these techniques help to probe the electronic structure directly.<sup>6,7,8</sup> The experimental results were simulated using configuration interaction (CI) calculations for the cluster of CoO<sub>6</sub> octahedron. All these investigations inferred the presence of varying mixtures of LS and HS states above 100 K.

Subsequently, a detailed study<sup>9</sup> based on LDA+*U* (LDA = local density approximation and *U* = electron-electron Coulomb repulsion strength) calculations, attributed the 100 K transitions to LS to orbital ordered intermediate spin (IS) state ( $t_{2g}^5 e_g^1 \Rightarrow S = 1$ ) and the one at 500 K to orbital disordered IS state as the energy of the latter state was found to be higher than the former and lower than HS state. Since then, numerous experimental and theoretical works have been carried out, which attributed the first transition to LS to IS state.<sup>12,13,14,15,16,17,18</sup> This has also been demonstrated

by PES and XAS studies,<sup>19</sup> where Co 2*p* core level, valence band and O *K*-edge XAS spectra of LaCoO<sub>3</sub> revealed 70% LS and 30% IS states in the temperature range 100 K to 300 K. No contribution of HS state was observed up to 300 K.

Recently, based on GGA+*U* (GGA = generalized gradient approximation) calculations, Knížek *et al.* showed that the mixed LS-HS state (1:1) is the first excited state and thus attributed the first magnetic transition from LS to LS-HS state.<sup>20</sup> This is in sharp contrast to the belief of IS contributions in the intermediate temperature range. In addition, experimental results based on XAS and magnetic circular dichroism<sup>21</sup> and inelastic neutron scattering<sup>22</sup> also interpreted in terms of mixed LS-HS state in the temperature range up to 700 K considering cluster approximations. It is, thus, evident that the spin state of Co at different temperatures is still controversial.

In this work, we investigate the spin state of Co in LaCoO<sub>3</sub> at room temperature using state-of-the-art photoemission spectroscopy and *ab initio* band structure calculations. We observe that spin-orbit coupling (SOC) plays an important role in determining the electronic structure in this system. The comparison of the high resolution spectra and the calculated results suggest that the electronic structure of LaCoO<sub>3</sub> at room temperature has large IS contributions. The *ab initio* calculations also provide a good representation of the experimental La 5*p* and O 2*s* core level spectra.

## II. EXPERIMENTAL AND COMPUTATIONAL DETAILS

Single crystal of LaCoO<sub>3</sub> was grown and characterized as described elsewhere.<sup>23</sup> The photoemission spectra of the valence band and shallow core levels were

recorded at room temperature (RT) using a spectrometer equipped with monochromatic Al  $K\alpha$  (1486.6 eV) and He I (21.2 eV) sources, and a Gammadata Scienta analyzer, SES2002. The base pressure during the measurements was about  $4 \times 10^{-11}$  Torr. The energy resolution for the  $x$ -ray photoemission was set to 0.3 eV for the valence band and 0.6 eV for the core level spectra. The resolution for the He I spectrum was fixed to 4 meV. The sample was cleaned *in situ* by scraping the sample surface using a diamond file. The cleanliness of the sample was ascertained by tracking the sharpness of O 1s peak and absence of C 1s peak. The Fermi level was aligned by recording the valence band spectrum of an Ag foil mounted on the same sample holder.

The LDA+ $U$  and GGA+ $U$  ( $U$  represents the electron correlation strength among Co 3d electrons), spin-polarized density of states (DOS) calculations were carried out using LMTART 6.61 (Ref. 24). For calculating charge density, full-potential linearized Muffin-Tin orbital (LMTO) method working in plane wave representation was employed. In the calculation, we have used the Muffin-Tin radii of 3.515, 2.005, and 1.64 a.u. for La, Co and O, respectively. The charge density and effective potential were expanded in spherical harmonics up to  $l = 6$  inside the sphere and in a Fourier series in the interstitial region. The initial basis set included 6s, 5p, 5d, and 4f valence, and 5s semicore orbitals of La; 4s, 4p, and 3d valence, and 3p semicore orbitals of Co, and 2s and 2p orbitals of O. The exchange correlation functional of the density functional theory was taken after H.S. Vosko *et al.* (Ref. 25) and GGA calculations are performed following J.P. Perdew *et al.* (Ref. 26). The calculations were performed by taking LS, IS and HS configurations, which correspond to  $(t_{2g}^3 t_{2g\downarrow}^3)$ ,  $(t_{2g}^3 t_{2g\downarrow}^2 e_{g\uparrow}^1)$  and  $(t_{2g}^3 t_{2g\downarrow}^1 e_{g\uparrow}^2)$  electronic configurations, respectively as initial input. Self-consistency was achieved by demanding the convergence of the total energy to be smaller than  $10^{-4}$  Ryd/cell. Final orbital occupancies for Co  $t_{2g}$  and  $e_g$  states were obtained from self-consistent GGA+ $U$  calculations for different initial state configurations. (8, 8, 6) divisions of the Brillouin zone along three directions for the tetrahedron integration were used to calculate the DOS.

### III. RESULTS AND DISCUSSIONS

It is well known that although the electron correlation effects are underestimated in *ab initio* band structure calculations within LDA, these results are often found to explain most of the features in PES and XAS results in transition metal oxide systems.<sup>27,28,29,30,31</sup> However, one needs to consider the correlation effects to capture the details of the spectra and the ground state properties of the system. We have calculated various contributions in the DOS of LaCoO<sub>3</sub> using both LDA and LDA+ $U$  methods. In order to minimize uncertainty in the calculated results, we have fixed the value of  $U$  to the experimen-

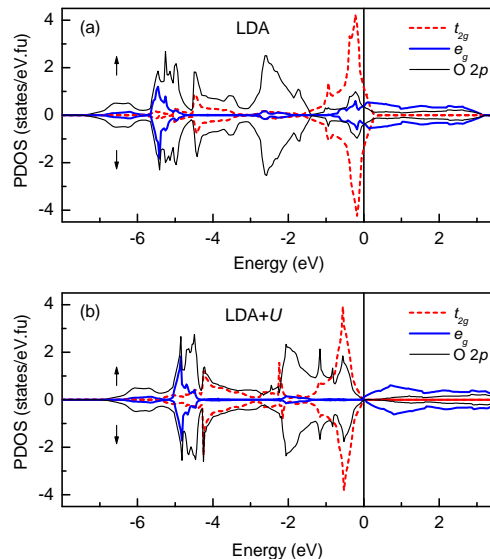


FIG. 1: (color online) O 2p (thin solid line) and Co 3d partial density of states having  $t_{2g}$  (dashed line) and  $e_g$  (thick solid line) symmetries from (a) LDA and (b) LDA+ $U$  calculations.

tally estimated values of 3.5 eV.<sup>32</sup>

In Fig. 1(a), we show the calculated LDA results for both the up and down spin states. There are several features observed in different energy positions. The features between -1.5 eV to -3 eV energies are dominated by the O 2p states with negligible contribution from other electronic states. These features are identified as O 2p non-bonding states. The features at lower energies have dominant contributions from O 2p electronic states with small but finite intensities from the Co 3d states having  $t_{2g}$  and  $e_g$  symmetries. Thus, the features between -3 to -4.5 eV can be attributed to bonding states with  $t_{2g}$  symmetry and those below -4.5 eV are the bonding states with  $e_g$  symmetry. The antibonding features appear above -1.5 eV and have predominantly Co 3d character. Co 3d bands with  $t_{2g}$  symmetry appear between -1.5 to 0.5 eV and the  $e_g$  bands between -1 to 3 eV. It is evident that the density of states at the Fermi level is large suggesting a metallic phase in the ground state in contrast to the insulating phase observed in various experiments.

The effect of electron correlation in the density of states is manifested in the LDA+ $U$  results as shown in Fig. 1(b). Although electron correlation among O 2p electrons is not considered in the calculations, the energy distribution of the O 2p partial density of states (PDOS) appears to be somewhat different from the LDA results. The O 2p contribution in the antibonding region appears to enhance in the LDA+ $U$  results compared to the LDA results suggesting a spectral weight transfer from the bands having bonding character. The non-bonding O 2p contributions also shift toward the Fermi level. The changes in the Co 3d bands are most significant as expected. The bonding and antibonding  $e_g$

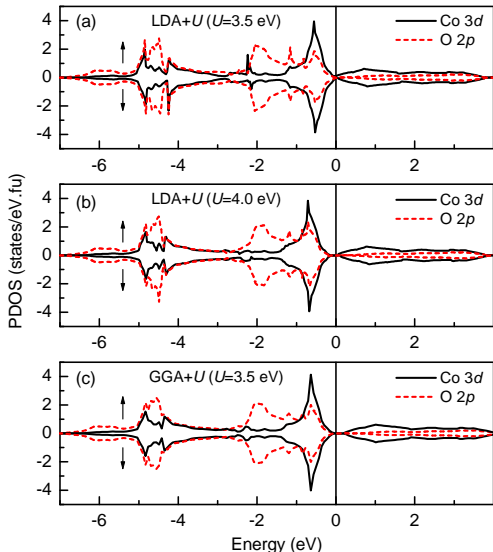


FIG. 2: (color online) Co 3d and O 2p partial density of states calculated using (a) LDA+ $U$  ( $U = 3.5$  eV), (b) LDA+ $U$  ( $U = 4$  eV) and (c) GGA+ $U$  ( $U = 3.5$  eV) methods.

bands shift towards higher energies. The bonding  $t_{2g}$  band appears almost at the same energies along with a significant increase in the spectral weight. Subsequently, the antibonding  $t_{2g}$  band having primarily Co 3d character becomes narrower along with a reduction in spectral weight. It is, thus, clear that consideration of  $U$  in the calculations leads to a decrease in Co 3d character and an increase in O 2p character of the bands in the vicinity of the Fermi level. Although the overlap between the  $t_{2g}$  and  $e_g$  band is minimized for these parameters, no hard gap is observed characterizing the systems to be metallic.

In order to investigate the value of  $U$  that creates a gap at the Fermi level, we compare the Co 3d and O 2p PDOS for  $U = 3.5$  eV and 4 eV in Fig. 2(a) and 2(b), respectively. It is evident that, an increase in  $U$  to 4 eV generates a band gap of about 0.2 eV. The shape and energy distribution of the DOS is almost the same in both the cases. The GGA is known to provide a better description of the exchange-correlation functional as it also considers first order correction to the spatial distribution of the electronic charge density used in the LDA calculations. In GGA, total energy of the system improves<sup>26</sup> and it is expected that the energy position of different bands would also improve. The calculated PDOS of Co 3d and O 2p corresponding to GGA+ $U$  calculations are shown in Fig. 2(c). In contrast to the metallic phase observed in LDA results, a value of  $U = 3.5$  eV creates a band gap of about 0.22 eV at the Fermi level in the results corresponding to GGA calculations, which is very close to that observed experimentally.<sup>33,34</sup> However, the shape and positions of Co 3d and O 2p bands is very similar in the LDA+ $U$  and GGA+ $U$  results. Thus, we used GGA+ $U$  method in the rest part of our study to discuss the experimental results.

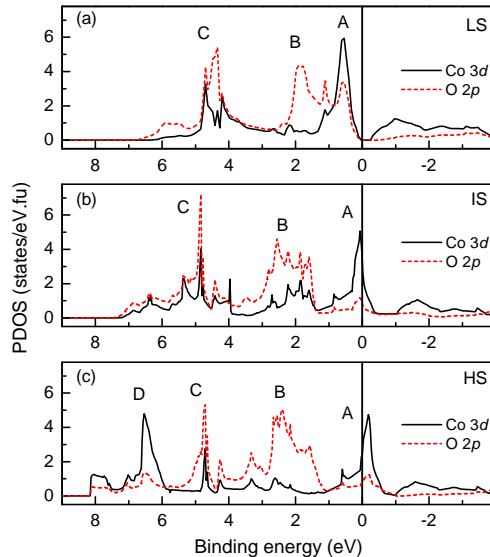


FIG. 3: (color online) Calculated Co 3d and O 2p partial density of states corresponding to low spin (LS), intermediate spin (IS) and high spin (HS) configurations using GGA+ $U$  method.

We now turn to the question of the influence of various spin states in the electronic structure of LaCoO<sub>3</sub>. The PDOS obtained for different spin state configurations are shown in Fig. 3 for the same values of  $U$  ( $= 3.5$  eV). It is evident that although the LS configuration leads to insulating ground state, the electronic structure corresponding to IS and HS configuration converges to metallic phase. This is a well know fact for this system and one needs to consider additional parameters such as orbital ordering to achieve insulating phase.<sup>9</sup> However, the energy distribution of the DOS over the large binding energy scale remains very similar. There are three distinctly separable features A, B and C in the DOS in Fig. 3. In the case of IS configuration, the  $t_{2g}$  band becomes partially filled. This effect enhances further in the case of HS configuration. The total intensity of the feature A gradually decreases with the change in spin state configuration from LS  $\rightarrow$  IS  $\rightarrow$  HS. In addition, the Co 3d character of the feature A becomes highest in the IS configuration (80.3%) while it is about 63.8% in the LS state and 64.8% in the HS state. The feature B representing the non-bonding O 2p states appears at slightly higher binding energies in the IS and HS states compared to that in the LS state. The change in the feature C is again substantial. The O 2p and Co 3d contributions are almost similar in LS and IS cases. In the case of HS states, the feature C has dominant O 2p character and a new feature D having dominant Co 3d character appears beyond 6 eV binding energies.

All the above calculations are done without considering the spin-orbit coupling (SOC) in any of the electronic states. Recently, there is a growing realization that SOC plays crucial role in determining the elec-

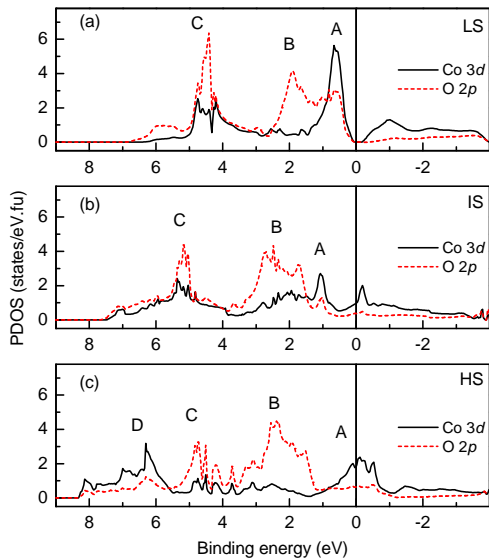


FIG. 4: (color online) Co 3d and O 2p partial density of states corresponding to low spin (LS), intermediate spin (IS) and high spin (HS) configurations calculated including spin-orbit interactions. All these calculations are performed using GGA+ $U$  method.

TABLE I: Occupancies of different Co 3d orbitals obtained from GGA+ $U$  calculations for low spin (LS), intermediate spin (IS) and high spin (HS) configurations of  $\text{Co}^{3+}$  in  $\text{LaCoO}_3$ . Numbers written in normal and bold face correspond to calculation without spin-orbit coupling and with spin-orbit coupling, respectively.

Initial spin state	$t_{2g\uparrow}$	$e_{g\uparrow}$	$t_{2g\downarrow}$	$e_{g\downarrow}$	Total
LS	2.77	0.58	2.77	0.58	6.7
	<b>2.77</b>	<b>0.59</b>	<b>2.77</b>	<b>0.58</b>	<b>6.71</b>
IS	2.79	1.5	1.95	0.43	6.67
	<b>2.8</b>	<b>1.36</b>	<b>2.03</b>	<b>0.45</b>	<b>6.64</b>
HS	2.82	1.9	1.32	0.42	6.46
	<b>2.83</b>	<b>1.9</b>	<b>1.35</b>	<b>0.41</b>	<b>6.49</b>

tronic structure in various transition metal oxides. The importance of SOC has been demonstrated in the systems possessing rare-earth 4f electrons.<sup>35</sup> In  $\text{Ca}_2\text{RuO}_4$ , it was shown that SOC plays an important role in the changeover of the spin and orbital anisotropy as a function of temperature.<sup>36</sup> Very recent theoretical studies of  $\text{Ca}_3\text{CoRhO}_6$  compound have shown that the insulating ground state can be achieved by considering SOC in the calculations.<sup>37</sup> In order to investigate the effect in the present case, we have calculated the PDOS in all the cases including SOC. The results are shown in Fig. 4. It is clear that SOC has no significant influence in the case of LS configuration. This is presumably due to the fact that all the energy bands are completely filled. The effect is most pronounced in Fig. 4(b) corresponding to IS state exhibiting a splitting of the sharp feature A.

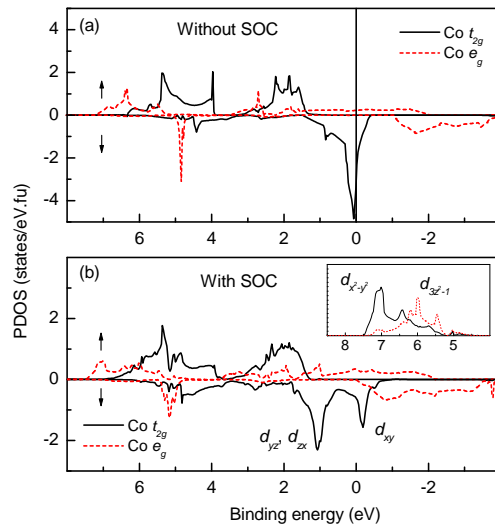


FIG. 5: (color online) Spin polarized partial density of states corresponding to Co  $t_{2g}$  and  $e_g$  bands calculated (a) without spin-orbit coupling and (b) with spin-orbit coupling. The inset shows  $d_{x^2-y^2}$  and  $d_{z^2}$  contributions in the  $e_{g\uparrow}$  band.

The effect of spin-orbit coupling in the occupancies of  $t_{2g\uparrow}$ ,  $e_{g\uparrow}$ ,  $t_{2g\downarrow}$ , and  $e_{g\downarrow}$  are given in Table 1. Numbers written in normal and bold face correspond to without SOC and with SOC, respectively. The total electronic occupancies of Co 3d bands corresponding to LS, IS and HS states are about 6.7, 6.65, and 6.47, respectively. These values are closer to those obtained from full-multiplet configuration interaction calculations carried out by Saitoh *et al.* (Ref. 19) and somewhat smaller from those obtained by Korotin *et al.* (Ref. 9). It is evident that the total occupancies as well as partial occupancies of  $t_{2g}$  and  $e_g$  orbitals corresponding to LS and HS states are not affected significantly by SOC. However, in IS state, the occupancies of  $e_{g\uparrow}$  orbitals decreases by 0.14 and that of  $t_{2g\downarrow}$  orbital increases by 0.08 due to the spin-orbit coupling keeping the total occupancy almost unchanged.

The details of the effect of SOC in the IS state are shown in Fig. 5, where we show the up and down spin PDOS of Co 3d bands separately. In Fig. 5(a), the feature in the vicinity of the Fermi level arises due to the down spin  $t_{2g}$  states. This feature splits into two distinctly separated features (the energy separation is about 1.2 eV). The feature at about 1 eV binding energy represents the doubly degenerate  $d_{xz}$  and  $d_{yz}$  bands and the non-degenerate  $d_{xy}$  band appears above the Fermi level. The doubly degenerate bonding  $e_{g\uparrow}$  band also splits by about 1 eV into  $d_{x^2-y^2}$  and  $d_{z^2}$  bands as shown in the inset of Fig. 5(b). It is thus clear that the degeneracy in the  $t_{2g}$  and  $e_g$  bands are partially lifted due to spin-orbit interactions and the effect is most pronounced in the IS configuration. Since, the  $d$  bands are not completely filled, the splitting of the  $t_{2g}$  and  $e_g$  bands will

TABLE II: Occupancies of  $3d$  orbitals in intermediate spin configuration of  $\text{Co}^{3+}$  in  $\text{LaCoO}_3$ . Numbers written in normal and bold face are corresponding to calculation without spin-orbit coupling and with spin-orbit coupling, respectively.

Spin	$d_{yz}$	$d_{zx}$	$d_{xy}$	$d_{x^2-y^2}$	$d_{z^2}$
Up	0.93	0.93	0.93	0.75	0.75
	<b>0.93</b>	<b>0.93</b>	<b>0.94</b>	<b>0.86</b>	<b>0.50</b>
Down	0.65	0.65	0.65	0.21	0.21
	<b>0.92</b>	<b>0.92</b>	<b>0.19</b>	<b>0.22</b>	<b>0.23</b>

influence the occupancy of these bands. Here, the SOC induced splitting leads to lowering in energy of  $d_{yz}$ ,  $d_{zx}$  and  $d_{x^2-y^2}$  bands and enhances the energy of  $d_{xy}$  and  $d_{z^2}$  bands. Thus, the occupancies of  $d_{yz}$ ,  $d_{zx}$  and  $d_{x^2-y^2}$  are expected to increase and that of  $d_{xy}$  and  $d_{z^2}$  to decrease. This is clearly manifested in the partial occupancies of each Co  $3d$  orbitals given in Table 2, where the occupancies of  $d_{yz\downarrow}$ ,  $d_{zx\downarrow}$  and  $d_{(x^2-y^2)\uparrow}$  increase by 0.27, 0.27 and 0.11, respectively, and that of  $d_{xy\downarrow}$  and  $d_{z^2\uparrow}$  decrease by 0.46 and 0.15, respectively.

In order to compare the calculated results with the experimental spectra, we show the background subtracted experimental valence band spectra at RT in Fig. 6. The spectra show three distinct features at about 1.0, 2.9 and 5.3 eV binding energies denoted by A, B and C, respectively. The relative intensity of various features are significantly different in the spectra using Al  $K\alpha$  and He I sources. While the feature A is most intense in the Al  $K\alpha$  spectrum, it becomes weakest in intensity in the He I spectrum. Subsequently, the intensities of the features B and C become dominant in the He I spectrum. It is well known that the photoemission cross section is very sensitive to the excitation energies.<sup>38</sup> While the cross section of O  $2p$  states is larger than that of Co  $3d$  states in the He I spectrum, the relative cross section becomes opposite in the Al  $K\alpha$  energies making the cross section for Co  $3d$  states significantly larger than that of O  $2p$  states. Thus, the changes in intensity of various features due to the change in excitation energy suggests that the feature A is predominantly contributed by Co  $3d$  states and the features B and C have large O  $2p$  character. No significant feature is observed between 6 to 8 eV binding energies. This clearly suggests that the experimental results are very similar to the results obtained for IS configuration shown in Fig. 4(b).

In order to bring out clarity to this comparison, we plot the O  $2p$  and Co  $3d$  PDOS corresponding to IS configuration in Fig. 6. The peak position of the feature B is somewhat higher (0.5 eV) in the experimental spectra compared to the calculated results. Such small shift in the completely filled non-bonding O  $2p$  bands has often been observed in the LDA results due to the underestimation of the electron correlation among the O  $2p$  electrons.<sup>27</sup> The energy positions of the features A and C in the experimental spectra, and the large Co  $3d$  character of the feature A and O  $2p$  character of feature C

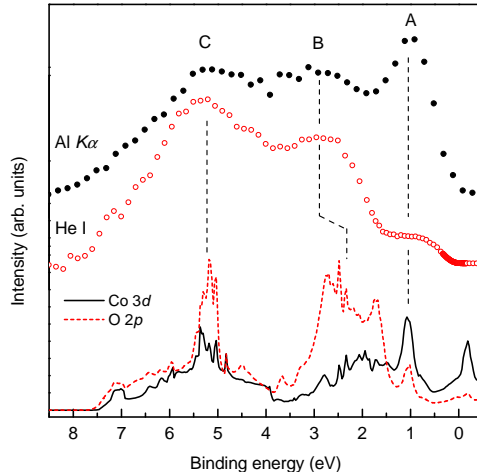


FIG. 6: (color online) Experimental valence band spectra collected at room temperature using Al  $K\alpha$  and He I radiations. The lines denote the calculated Co  $3d$  and O  $2p$  partial density of states corresponding to intermediate spin configuration of Co including spin-orbit coupling.

is revealed remarkably in the calculated results. Even the small shoulder in the binding energy range 5.5 - 7.5 eV with relatively larger O  $2p$  character is reproduced in the calculated results. These results clearly suggest that the electronic structure of  $\text{LaCoO}_3$  at room temperature corresponds primarily to the intermediate spin state configuration of Co and the contribution from HS state configuration may not be so significant. These results appear to be different from those in the recent studies based on cluster approximations.<sup>21</sup> Such difference may not be surprising as in the cluster calculations, the Co  $3d$  and O  $2p$  bands are approximated to atomic energy levels.

Finally, we investigate the applicability of *ab initio* band structure calculations in understanding the shallow core level spectrum. Such study will be quite interesting as core-hole potential is known to influence the final states of the core level photoemission. The integral background subtracted experimental spectrum along with the calculated one is plotted in Fig. 7(a). Three distinct features visible in the spectrum. The features at 16 and 18 eV binding energies correspond to spin-orbit split La  $5p$  states as marked in the figure. The feature around 21 eV binding energy represent the signature of photoemission from O  $2s$  levels.

We also show the La  $5p$  and O  $2s$  PDOS corresponding to LS, IS and HS configurations in different panels of Fig. 7. All the three features are present in the calculated results corresponding to LS, IS and HS states. The shape of the bands in each region remains almost the same in each spin state. The spin-orbit splitting of the La  $5p$  contributions in the PDOS is about 2 eV as also observed in the experimental spectra. However, the peak position of the bands corresponding to LS state appears at binding energies lower by about 1 eV in comparison to energies

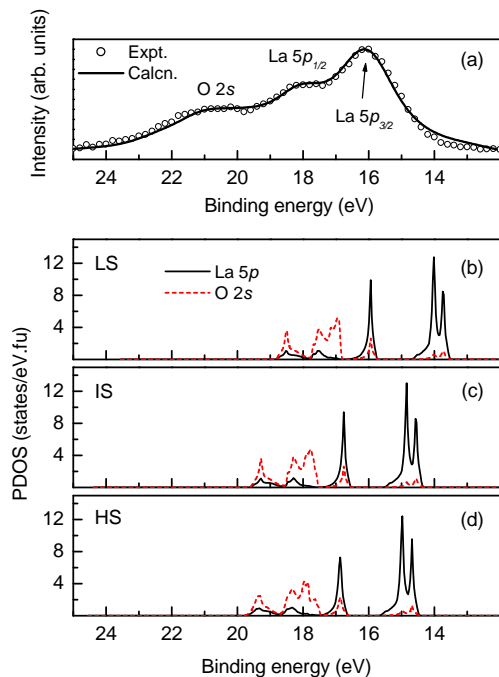


FIG. 7: (color online) (a) Background subtracted La  $5p$  and O  $2s$  core level spectra (symbols) collected at room temperature. The solid line represent the spectrum simulated using PDOS corresponding to IS state configuration. La  $5p$  (solid line) and O  $2s$  (dashed line) PDOS calculated using (b) LS, (c) IS and (d) HS configurations of Co.

corresponding to IS and HS states, which are closer to the experimental spectra.

In order to simulate the experimental spectrum, we have shifted the calculated O  $2s$  and La  $5p$  PDOS obtained from IS configuration by 3.1 eV and 1.2 eV, respectively and then multiplied by photoemission cross sections of the corresponding states.<sup>38</sup> To account for the lifetime broadening and resolution broadening, O  $2s$  and La  $5p$  PDOS are convoluted with a suitable Lorentzian and a Gaussian, respectively. The simulated spectrum is shown by solid line overlapped on the experimental spectrum in Fig. 7(a). The reproduction of the experimental spectrum is remarkable. This suggests that one

can indeed employ band structure calculations to determine the core level spectrum. It is to note here that these calculations cannot create features appearing due to different screening effects expected in the final state of photoemission. Almost perfect reproduction of the experimental spectrum in the present case indicates that final state effects may not be significant in the case of La  $5p$  photoemission.

#### IV. CONCLUSIONS

In summary, we have investigated the electronic structure of LaCoO<sub>3</sub> at room temperature using various forms of *ab initio* calculations and high resolution photoemission spectroscopy on high quality single crystal. We observe that GGA+*U* calculations provide a good description of the ground state. Spin-orbit coupling appears to play a significant role in the case of IS and HS states of Co, which is most pronounced in the case of IS state of Co. The calculated Co  $3d$  and O  $2p$  partial density of states corresponding to intermediate spin state of Co provide the best description of the experimental valence band spectra at room temperature. This suggests that the spin state of Co at room temperature presumably has dominant intermediate spin configuration and that the contribution from high spin state is not so significant at this temperature. The applicability of the *ab initio* band structure calculations in understanding the shallow core level spectrum is also studied. The calculated exchange splitting of La  $5p$  states is found to be about 2 eV, which is identical to the experimentally observed splitting. The lineshape of the calculated spectrum provides a good description of the experimental spectrum. This suggests that final state effects may not be significant in the case of La  $5p$  photoemission in LaCoO<sub>3</sub>.

#### V. ACKNOWLEDGEMENTS

The authors would like to thank Prof. A. V. Narlikar for continued support. SP is thankful to CSIR, India, for financial support.

<sup>1</sup> J.B. Goodenough, J. Phys. Chem. Solids **6**, 287 (1958).  
<sup>2</sup> R.R. Heikes, R.C. Miller, and R. Mazelsky, Physica **30**, 1600 (1964).  
<sup>3</sup> P.M. Raccah and J.B. Goodenough, Phys. Rev. **155**, 932 (1967).  
<sup>4</sup> V.G. Bhide, D.S. Rajoria, and Y.S. Reddy, Phys. Rev. Lett. **28**, 1133 (1972).  
<sup>5</sup> B.W. Veal and D.J. Lam, J. Appl. Phys. **49**, 1461 (1978).  
<sup>6</sup> M. Abbate, J.C. Fuggle, A. Fujimori, L.H. Tjeng, C.T. Chen, R. Potze, G.A. Sawatzky, H. Eisaki, and S. Uchida, Phys. Rev. B **47**, 16124 (1993).  
<sup>7</sup> S. R. Barman and D. D. Sarma, Phys. Rev. B **49**, 13979

(1994).  
<sup>8</sup> D. J. Lam, B. W. Veal, and D. E. Ellis, Phys. Rev. B **22**, 5730 (1980)  
<sup>9</sup> M. A. Korotin, S. Yu. Ezhov, I. V. Solovyev, V. I. Anisimov, D. I. Khomskii, and G. A. Sawatzky, Phys. Rev. B **54**, 5309 (1996).  
<sup>10</sup> V. P. Plakhty, P. J. Brown, B. Grenier, S. V. Shiryaev, S. N. Barilo, S. V. Gavrilov, and E. Ressouche, J. Phys.: Condens. Matter **18**, 3517 (2006).  
<sup>11</sup> S. Yamaguchi, Y. Okimoto, H. Taniguchi, and Y. Tokura, Phys. Rev. B **53**, R2926 (1996).  
<sup>12</sup> Y. Kobayashi, N. Fujiwara, S. Murata, K. Asai, and H.

- Yasuoka, Phys. Rev. B **62**, 410 (2000).
- <sup>13</sup> C. Zobel, M. Kriener, D. Bruns, J. Baier, M. Grüninger, T. Lorenz, P. Reutler, and A. Revcolevschi, Phys. Rev. B **66**, 020402(R) (2002).
- <sup>14</sup> P.G. Radaelli and S.W. Cheong, Phys. Rev. B **66**, 094408 (2002).
- <sup>15</sup> G. Maris, Y. Ren, V. Volotchaev, C. Zobel, T. Lorenz, and T. T.M. Palstra, Phys. Rev. B **67**, 224423 (2003).
- <sup>16</sup> I.A. Nekrasov, S.V. Streltsov, M.A. Korotin, and V.I. Anisimov, Phys. Rev. B **68**, 235113 (2003)
- <sup>17</sup> A. Ishikawa, J. Nohara, and S. Sugai, Phys. Rev. Lett. **93**, 136401 (2004)
- <sup>18</sup> D. Phelan, D. Louca, S. Rosenkranz, S.-H. Lee, Y. Qiu, P.J. Chupas, R. Osborn, H. Zheng, J.F. Mitchell, J.R.D. Copley, J.L. Sarrao, and Y. Moritomo, Phys. Rev. Lett. **96**, 027201 (2006).
- <sup>19</sup> T. Saitoh, T. Mizokawa, A. Fujimori, M. Abbate, Y. Takeda, and M. Takano, Phys. Rev. B **55**, 4257 (1997)
- <sup>20</sup> K. Knížek, Z. Jirák, J. Hejtmánek, and P. Novák, J. Phys.: Condens. Matter **18**, 3285 (2006).
- <sup>21</sup> M. W. Haverkort, Z. Hu, J. C. Cezar, T. Burnus, H. Hartmann, M. Reuther, C. Zobel, T. Lorenz, A. Tanaka, N. B. Brookes, H. H. Hsieh, H.-J. Lin, C. T. Chen, and L. H. Tjeng, Phys. Rev. Lett. **97**, 176405 (2006)
- <sup>22</sup> A. Podlesnyak, S. Streule, J. Mesot, M. Medarde, E. Pomjakushina, K. Conder, A. Tanaka, M. W. Haverkort, and D. I. Khomskii, Phys. Rev. Lett. **97**, 247208 (2006)
- <sup>23</sup> D. Prabhakaran, A. T. Boothroyd, F. R. Wondre, and T. J. Prior, J. Cryst. Growth **275**, e827 (2005)
- <sup>24</sup> S. Y. Savrasov, Phys. Rev. B **54**, 16470 (1996), S. Y. Savrasov, cond-mat/0409705
- <sup>25</sup> S. H. Vosko, L. Wilk, and M. Nusair, Can. J. Phys. **58**, 1200 (1980)
- <sup>26</sup> J. P. Perdew, K. Burke, and M. Ernzerhof, Phys. Rev. Lett. **77**, 3865 (1996)
- <sup>27</sup> D.D. Sarma, N. Shanthi, S.R. Barman, N. Hamada, H. Sawada, and K. Terakura, Phys. Rev. Lett. **75**, 1126 (1995).
- <sup>28</sup> Kalobaran Maiti, Phys. Rev. B **73**, 115119 (2006).
- <sup>29</sup> K. Maiti and R.S. Singh, Phys. Rev. B **71**, 161102(R) (2005).
- <sup>30</sup> S. K. Pandey, Ashwani Kumar, S. M. Chaudhari, and A. V. Pimpale, J. Phys.: Condens. Matter **18**, 1313 (2006)
- <sup>31</sup> S. K. Pandey, S. Khalid, and A. V. Pimpale, J. Phys.: Condens. Matter **19**, 036212 (2007)
- <sup>32</sup> A. Chainani, M. Mathew, and D.D. Sarma, Phys. Rev. B **46**, 9976 (1992).
- <sup>33</sup> T. Arima, Y. Tokura, and J. B. Torrance, Phys. Rev. B **48**, 17006 (1993)
- <sup>34</sup> E. Iguchi, K. Ueda, and W. H. Jung, Phys. Rev. B **54**, 17431 (1996)
- <sup>35</sup> T. Hotta, Rep. Prog. Phys. **69**, 2061 (2006).
- <sup>36</sup> T. Mizokawa, L.H. Tjeng, G.A. Sawatzky, G. Ghiringhelli, O. Tjernberg, N.B. Brookes, H. Fukazawa, S. Nakatsuji, and Y. Maeno, Phys. Rev. Lett. **87**, 077202 (2001).
- <sup>37</sup> H. Wu, Z. Hu, D.I. Khomskii and L.H. Tjeng, Phys. Rev. B **75**, 245118 (2007).
- <sup>38</sup> J. J. Yeh and I. Lindau, At. Data Nucl. Data Tables **32**, 1 (1985)